

SYNTHESIS OF ULTRAFINE (Mo,W)Si₂ COMPOSITE POWDERS FROM HIGH PURITY MOLYBDENUM CONCENTRATE

J.-B. Huang, G.-H. Zhang*

State Key Laboratory of Advanced Metallurgy, University of Science and Technology Beijing, Beijing, China.

(Received 25 May 2023; Accepted 19 December 2023)

Abstract

(Mo,W)Si₂ composite powders with the grain size of about 1 μm were synthesized at 1150°C for 2 h. The high purity molybdenum concentrate (with the main component of MoS₂), W and Si powders were utilized as raw materials and lime as desulfurizer. The graphite felt was laid between the compact (made of MoS₂, W and Si) and the lime to facilitate the separation of the produced composite powders from desulfurization product. The phase composition, microstructure evolution, and residual sulfur content during the silicothermic reduction reaction were evaluated. The experimental results showed that the reaction could be completed after a reaction time of 1150 °C for 2 h, and the residual sulfur content of the product was 0.087 wt.%. It was concluded that the interactions between Si and the intermediate products of SiS and SiS₂ are crucial for the preparation of (Mo,W)Si₂ composite powders at low temperatures. The preparation process could be divided into three stages: solid state reactions between MoS₂, W and Si to produce MoSi₂, WSi₂ and gaseous SiS; gas-solid reaction between MoS₂, W and gaseous SiS to generate MoSi₂, WSi₂ and gaseous SiS₂; and gas-solid reaction between gaseous SiS₂ and Si to form SiS gas. With this short flow process, fine-grained (Mo,W)Si₂ composite powders can be produced at low cost at low temperature, which has great application potential.

Keywords: Molybdenum disilicide; Tungsten disilicide; Composite powders; Silicothermic reduction

1. Introduction

Molybdenum disilicide (MoSi₂) has attracted considerable interest owing to its high melting point (above 2000°C), moderate density (about 6.28 g/cm³) and excellent thermal/electrical conductivity. Other advantages include dramatic oxidation and corrosion resistance in oxidizing atmospheres, primarily due to a thin, coherent, adherent, and protective silica layer that forms on the surface. MoSi₂ is now used in many applications, such as heating elements, high temperature oxidation resistant coating materials, aerospace gas turbine engines and industrial gas burners. However, monolithic MoSi₂ has weak fracture toughness at room temperature and low strength at high temperatures (above 1000°C) [1-7]. Hence, many studies have been carried out in recent years to improve the mechanical characteristics of MoSi₂-based materials by fine grain strengthening and nanoparticle reinforcement [8,9]. MoSi₂ has thermodynamic stability with numerous carbides, nitrides, oxides, and boride ceramic reinforcements such as SiC, Si₃N₄, ZrO₂, Al₂O₃, Y₂O₃ and ZrB₂ at high temperatures [1,10-19]. It has been demonstrated that the addition of a second phase can improve hardness, fracture toughness and bending strength could be

achieved by adding a second phase. In addition, alloying elements such as Al, Cr, W, V and Ta have been used to improve the mechanical properties [20-23]. Since both Mo and W belong to the VIB group, and WSi₂ is most similar to MoSi₂ in terms of crystal structure, alloying MoSi₂ with WSi₂ can significantly improve the overall performance [24-26]. Zhang et al. [24] reported that the MoSi₂-based composite with 50 mol.% WSi₂ has fracture toughness about 86% higher than that of monolithic MoSi₂. Similarly, Chen et al. [25] investigated WSi₂ reinforced MoSi₂ composites and found that a MoSi₂ matrix with 5 vol.% WSi₂ sample exhibited the optimum mechanical properties. Bose et al. [26] illustrated that alloying MoSi₂ with WSi₂ significantly reduced the high-temperature creep of MoSi₂.

Due to the high melting points of MoSi₂ and WSi₂ (2030°C and 2165°C, respectively) the powder sintering method is generally used for preparing MoSi₂-WSi₂ composites. Thus, a powder with fine particle size and homogeneous composition is the foundation for the production of high-performance MoSi₂-based composite materials. MoSi₂/WSi₂ powders were produced by mechanical alloying (MA) [27,28], the self-propagating high-temperature synthesis method (SHS) [29], the solid phase

Corresponding author: ghzhang0914@ustb.edu.cn

<https://doi.org/10.2298/JMMB230525041H>



replacement method [30] and plasma spray processing [31]. Schwarz et al. [27] synthesized MoSi_2 composite powders with different W contents from elemental powders by MA. Zamani et al. [28] fabricated the $(\text{Mo,W})\text{Si}_2$ - WSi_2 nanocomposite by MA. It should be noted that long-term ball milling inevitably introduces impurities into the product. Jo et al. [29] prepared MoSi_2 powder by SHS using Mo and Si powders as primary materials. Even though lots of efforts have been made, most studies in the literature selected Mo and W powders as the molybdenum and tungsten source, respectively.

It is worth mentioning that the grain size of the powder has a considerable impact on the sintering activity [9]. However, it is difficult to prepare ultrafine Mo powder by the normal hydrogen reduction process due to the presence of chemical vapor transport (CVT) mechanism, which limits the production of ultrafine MoSi_2 powder with low cost. Generally, the Mo element occurs naturally in the form of sulfide minerals, which can be easily purified to get MoS_2 [32-34]. Molybdenite concentrate is an essential ore mineral in the molybdenum industry for the production of molybdenum. Firstly, molybdenite concentrate is oxidation roasted to produce commercial molybdenum oxides. Secondly, the ammonium molybdate is prepared via ammonia leaching of commercial molybdenum oxides. Thirdly, the ammonium molybdate is oxidation roasted to generate pure MoO_3 . Finally, pure MoO_3 is reduced to MoO_2 and then to Mo by H_2 . As discussed above, the preparation of Mo is complicated and involves high-energy consumption, resulting in relatively high costs. On the contrary, the cost of pure MoS_2 powder, which can be prepared from molybdenite concentrate after acid leaching, is much lower than that of pure Mo powder.

Therefore, it would be both energy and cost saving if MoS_2 could be directly used as the molybdenum source to prepare MoSi_2 . In a previous study [35], it was proposed that MoSi_2 powder can be successfully prepared by silicothermic reduction of MoS_2 , which could significantly reduce the production cost. Meanwhile, a sulfur-emission free route was also used to treat sulfur-containing by-products during the silicothermic reduction process [36].

Hence, the aim of this work is to synthesize ultrafine MoSi_2 - WSi_2 composite powders by silicothermic reduction method using high purity molybdenum concentrate (MoS_2), Si and W powders as raw materials. The samples were coated with desulfurizer (CaO) to capture the sulfur-containing gaseous by-product. The phase transition, microstructure evolution, residual sulfur content and reaction mechanism during the silicothermic reduction reaction process were evaluated in detail.

2. Experiment details

In this study, high purity molybdenite concentrate (MoS_2 , 98.5 % purity, average size of about 2 μm), Si (99.99 % purity, average size of about 5 μm) and W powder (99 % purity, average size of about 300 nm) were used as raw materials, with corresponding morphologies shown in Figures 1(A-C). Calcium carbonate (CaCO_3 , 99% purity) was pyrolyzed at 1000 $^\circ\text{C}$ for 10 h to create lime powder (CaO), which was then utilized as a desulfurizer.

W powder was prepared via a two-stage reduction approach of WO_3 [37]. The powders of MoS_2 , Si and W were accurately weighed and homogeneously mixed in a mortar with alcohol as the medium according to the desired stoichiometric composition. The slurry was dried in an oven at 90 $^\circ\text{C}$ for 30 min. Following that, about 5 g of the as-mixed powder was pressed into a cuboid stainless steel mold under a uniaxial charge of 64 MPa for 5 min. The compositions and nomenclatures of different powder mixtures are summarized in Table 1. For comparison, powders of Mo, W, and Si are also used to directly synthesize MoSi_2 - WSi_2 composite powder.

The green compact was precisely weighed and then put in an alumina crucible. In order to easily remove the target product from desulfurized layer after the reaction, graphite felt was laid between the green compact and the desulfurizer lime. The quality of the added lime was 1.5 times the theoretical consumption calculated by reaction (1). When the temperature reached the designated temperature (1100 $^\circ\text{C}$ or 1150 $^\circ\text{C}$), the quartz tube with the sample was inserted into the furnace chamber and kept under the argon atmosphere (Ar, 200 ml/min) for various periods of

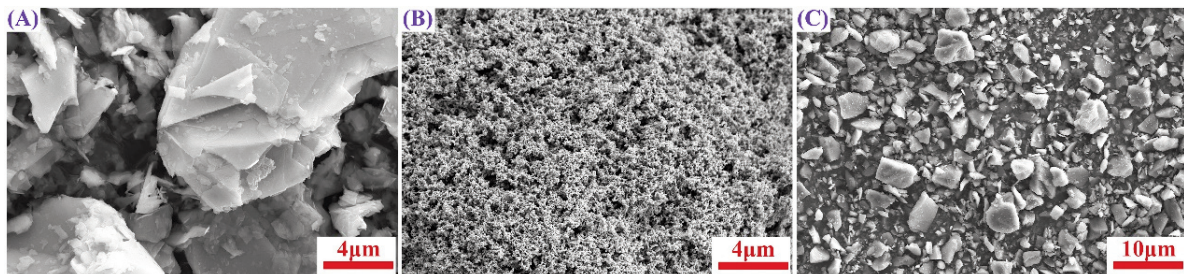
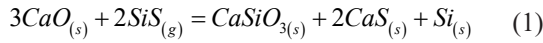


Figure 1. Morphologies of the raw materials of (A) MoS_2 , (B) W, and (C) Si

Table 1. The compositions and nomenclature of studied samples (mol.%)

Samples	MoS ₂	W	Si	Materials
MWS0	100	0	200	MoSi ₂
MWS1	97.5	2.5	200	MoSi ₂ -2.5 mol.%WSi ₂
MWS2	95	5	200	MoSi ₂ -5 mol.%WSi ₂
MWS3	90	10	200	MoSi ₂ -10 mol.%WSi ₂

time. Once the reaction was finished, the sample was removed and allowed to cool naturally to room temperature. The target product was accurately weighed again to calculate the mass loss. Then, the bulk product was crushed into powder and sieved through a 200-mesh sieve for the subsequent analysis.



To determine the phase composition, X-ray diffraction analysis (XRD, TTR III, Rigaku Corporation, Japan) was performed, with Cu K α radiation in the 2 θ range of 10-90°, a scan rate of 0.2 s/step and a step-size of 0.02 deg/step. The microstructures of the raw materials and the obtained composite powders were characterized by field-emission scanning electron microscopy (FE-SEM, ZEISS SUPRA 55, Oberkochen, Germany) with an energy dispersive X-ray spectrometer (EDS). The residual sulfur content of the sample was measured by an infrared carbon-sulfur analyzer (EMIA-920V2; HORIBA).

3. Results and discussion

After the reaction, the surface of the desulfurization layer remained white (color of CaO), indicating that the sulfur-containing by-products were completely captured. Clearly, there is a classic sandwich structure (top desulfurization layer-graphite felt-products). Due to the presence of graphite felt as an intermediate layer, the product layer can be easily removed from the desulfurization layer. Simultaneously, due to the porous characteristics of the graphite felt, the SiS gas can cross the graphite felt and react with CaO. Meanwhile, the graphite felt is not involved in any reaction and can be used repeatedly.

3.1. Thermodynamic analyses

The main reactions for the preparations of MoSi₂-WSi₂ composite powders could be described by Eqs. (2-3). The changes in the standard Gibbs free energy of these two reactions with temperature are indicated in Figure 2. Obviously, the changes of standard Gibbs free energy of Eqs. (2-3) are all negative in the temperature range of 1100-1150°C, suggesting that

these reactions are all possible from the viewpoint of thermodynamics. However, the initial reaction should occur between the solid MoS₂ and solid Si since the reaction temperature is lower than the melting points of the two.

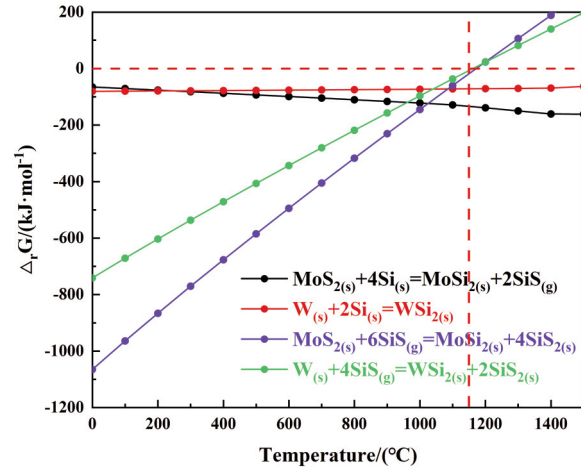
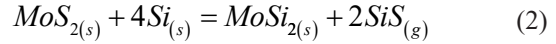
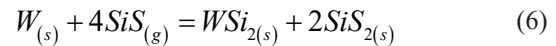
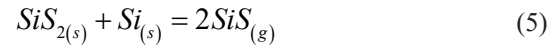


Figure 2. Temperature dependences of the changes of standard Gibbs free energy for different reactions

According to previous work [36,38,39], the SiS produced in reaction (2) was not directly captured by the top layer of CaO. The produced SiS is a gaseous phase above 1100°C and reacts with the nearby MoS₂ immediately (reaction 4). Simultaneously, the formed SiS₂ transfers to the surface of the Si particle to react and produce gaseous SiS again which participates in the MoSi₂ formation process (reaction 5). According to Figure 2, the change in standard Gibbs free energy of reaction (4) at temperatures ranging from 1100°C to 1150°C is higher than that of reaction (2). However, when gaseous SiS participate in the process, the mass transfer rate increases considerably.



Furthermore, reaction (6) is also a gas-solid reaction with a negative standard Gibbs free energy change in the temperature range of 1100-1150°C. Another experiment was carried out to investigate the feasibility of reaction (6) at 1150°C. Firstly, a green compact (about 4 g) consisting of MoS₂ and Si mixture with a molar ratio of 4:1 was placed on the



left side of the alumina crucible to offer SiS gas, and about 0.2 g of W powder was placed on the other side. Then, the crucible was covered with a graphite sheet to ensure that the SiS gas generated by reaction (2) could contact and react with the W powders on the right side. The quartz tube with the alumina crucible was heated for 2 h in argon atmosphere when the temperature reached 1150°C. Figure 3(A) illustrates the schematic diagram of the verification experiment. Finally, the products on the right side of the crucible were characterized, and their XRD results were plotted in Figure 3(B). Obviously, both W_5Si_3 (PDF 51-941) and SiS_2 (PDF 47-1375) can be confirmed after reacting at 1150°C for 2 h, which reveals that the formed gaseous SiS can react with W, as represented by reaction (6). The reason for the occurrence of W_5Si_3 can be explained as the insufficient contact in the gas-solid interaction between W and SiS(g), the reaction between W and SiS is not complete. Thus, many silicon-poor phases (W_5Si_3) and unreacted W are detected in the XRD patterns of the product. In summary, the method for synthesizing $MoSi_2$ - WSi_2 composite powders from MoS_2 , Si and W powders by silicothermic reduction is thermodynamically feasible.

Interestingly, the relationship between SiS, Si and SiS_2 is similar to the relationship with CO, C and CO_2 during the ironmaking process in high blast furnace, as described by Eqs. (7-9). SiS plays the same role as CO, while Si and SiS_2 play the same role as C and CO_2 , respectively. In the top part of the blast furnace, most of the reactions are carried out by reaction (8). This is comparable to the current experimental situation.



It should be pointed out that not all the generated SiS reacts with MoS_2 and W. A part of them escapes from the product layer and are captured by the surface-covered CaO. The desulfurization reaction between CaO and SiS is a highly exothermic process with a great enthalpy change of about -874 KJ/mol at 1150°C, which is of great significance to the process of preparing composite powders at low temperatures. Firstly, the sulfur-containing by-products are not

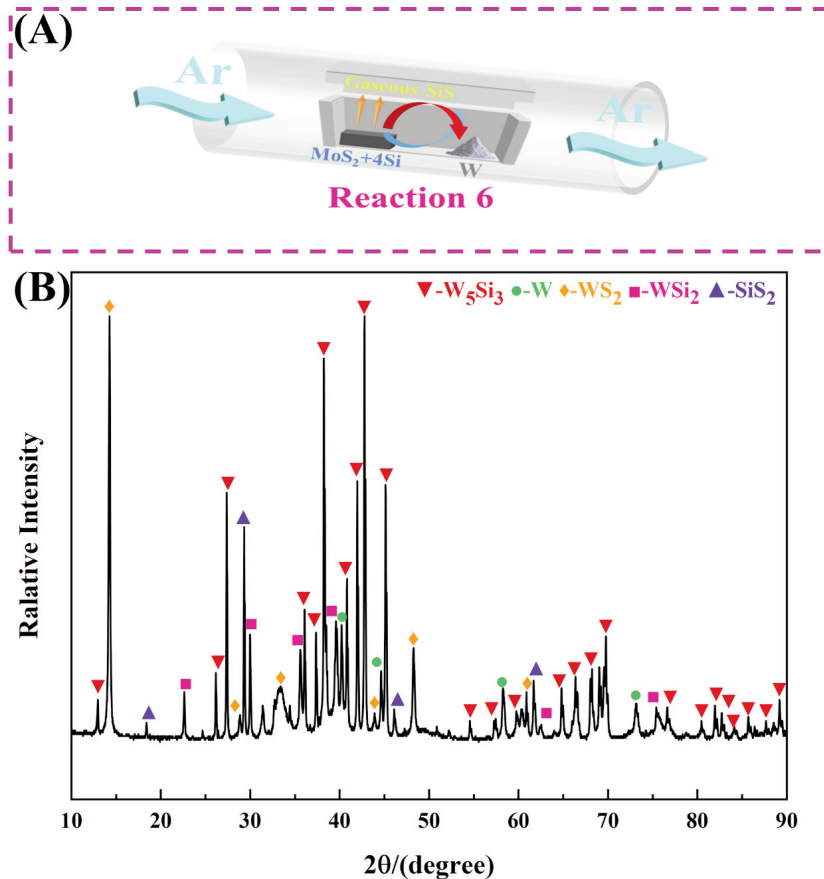


Figure 3. (A) Schematic diagram of reaction between SiS and W, (B) The XRD patterns of reaction product of W

released and do not cause environmental pollution. Next, a large amount of heat generated by the desulfurization reaction (reaction 1) can accelerate the reaction but it could also lead to the grain size growth.

3.2. Phase analysis of products prepared under different reaction temperatures and times

Figure 4(A) illustrates the XRD patterns of products with different W contents obtained after reacting at 1100°C for 2 h. The powder diffraction data, including PDF 41-0612 (MoSi_2), PDF 44-1055 (WSi_2), PDF 49-1491 $(\text{Mo,W})\text{Si}_2$, PDF 89-3659 (W), were used to identify crystalline phases. Clearly, the main phases of the products are $(\text{Mo,W})\text{Si}_2$, WSi_2 and a small amount of unreacted W. The diffraction peak of Si disappears completely under the present conditions. Besides, the sulfur-containing phase cannot be detected in all samples, which shows that MoS_2 and Si were completely reacted. It should be stated that the main products are $(\text{Mo,W})\text{Si}_2$ and WSi_2 . It should be noted that, in contrast to Figure 3, the W_5Si_3 diffraction peak is not found. This is due to the fact that W thoroughly reacted with Si and gaseous SiS to form WSi_2 after pressing the raw materials into green compacts.

Both Mo and W have a body-centered cubic structure with nearly identical lattice parameters ($a_{\text{Mo}} = 3.14700 \text{ \AA}$ and $a_{\text{W}} = 3.16540 \text{ \AA}$), resulting in very close Bragg peaks that are difficult to distinguish [40]. Moreover, the similar lattice constants and identical tetragonal structures of the MoSi_2 and WSi_2 phases enable the potential for many Mo atoms to be

substituted by W atoms [24]. Figure 4(D) gives the drawings of yellow region enlargement in Figure 4(C). It can be clearly seen that the diffraction peaks of the MoSi_2 samples doped with W shift to a small angle compared to the MoSi_2 samples without W doped, indicating that the W atoms are dissolved in the MoSi_2 lattice. It is worth mentioning that the W powder used in this work is about 300 nm in size, as shown in Figure 1, which is conducive to the uniform distribution of W in the $(\text{Mo,W})\text{Si}_2$ composite powder. According to the chemical composition of the product, they can be labeled as $(\text{Mo}0.975,\text{W}0.025)\text{Si}_2$, $(\text{Mo}0.95,\text{W}0.05)\text{Si}_2$ and $(\text{Mo}0.9,\text{W}0.1)\text{Si}_2$, respectively. Additionally, the lattices of MoSi_2 and WSi_2 are so comparable that their diffraction peaks are extremely close to each other in XRD results. Therefore, MoSi_2 peaks cannot be found in XRD patterns. The same phenomenon has also been reported in the literature [41-43]. Stergiou et al. [41] also prepared $(\text{Mo,W})\text{Si}_2$ composite with a low W content (2.1 at% W), and the major phase present was MoSi_2 with W in solid solution according to the results of XRD and SEM-EDS. Furthermore, the diffraction peak of hexagonal WSi_2 is also observed. The only structural distinction between tetragonal WSi_2 ($a=0.321 \text{ nm}$, $c=0.786 \text{ nm}$) and hexagonal WSi_2 ($a=0.461 \text{ nm}$, $c=0.641 \text{ nm}$) is the stacking order: tetragonal- WSi_2 has an ABAB stacking sequence while hexagonal- WSi_2 has an ABCABC order [45]. Zamani et al. and Ovalı et al. [28,46,47] reported the formation of hexagonal WSi_2 during the fabrication of W silicides by MA. Based on the above analyses, the overall reaction taking place in the system can be

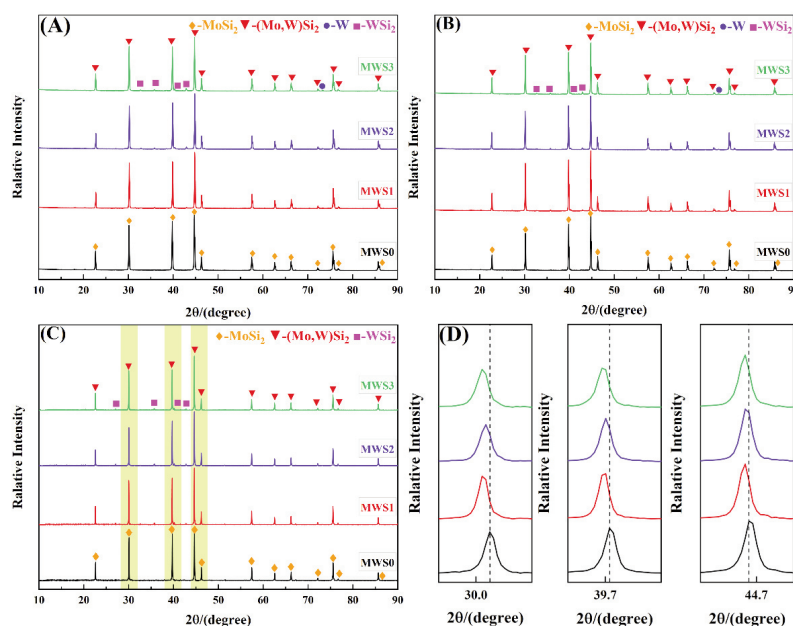
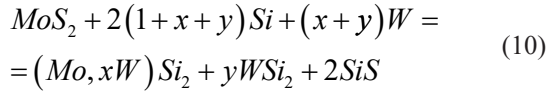


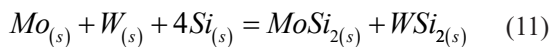
Figure 4. XRD patterns of products obtained at various conditions. (A) 1100°C, 2 h; (B) 1100°C, 4 h; (C) 1150°C, 2 h; (D) Drawings of yellow region enlargement in (C)

expressed in reaction (10). Moreover, the diffraction peak intensity of the hexagonal WSi_2 is obviously enhanced as W content increases.



The XRD patterns of resultant powders with various W contents obtained at 1100 °C for 4 hours are plotted in Figure 4(B). The peak intensity of WSi_2 is enhanced with the increase in W content. At the same time, the weak diffraction peak of W can still be observed. Figure 4(C) presents the XRD patterns of resultant powders with various contents of W obtained at 1150°C for 2 h. Only diffraction peaks for $(Mo,W)Si_2$ and WSi_2 are present. Thus, all reactants were reacted completely under the present conditions.

In the current method, MoS_2 , W and Si are used to prepare $(Mo,W)Si_2$ composite powders at very low temperature. In order to verify the advantages of this experimental system, reactions among Mo, W and Si powders were conducted at 1150°C for 2 h. In this case, Mo, W and Si powders were mixed according to the MWS3 composition. The experimental process was the same as the above experiments. The possible reaction of the system can be demonstrated as reaction (11), and the XRD result of the product is shown in Figure 5. The characteristic peaks of Mo (PDF 65-7442), W (PDF 89-3659) and Si (PDF 77-21108) can be observed, revealing that most of the raw materials do not react. Additionally, only a small amount of Mo_3Si (PDF 75-1182) was produced. It is worth noting that the reaction (11) has a negative change in standard Gibbs free energy at 1150°C. However, compared to the MoS_2 -W-Si system, there is no gaseous intermediate product in the Mo-W-Si system, which leads to a low reaction rate and extent. Generally, the current process has great advantages and enable the preparation of $(Mo,W)Si_2$ composite powders at low temperatures.



3.3. Weight loss investigation at temperature of 1150°C

The sample MWS3 was selected for further analysis in order to investigate the reaction process. Six cuboids (about 5 g) were reacted at 1150°C for 2, 5, 10, 15, 30 and 60 min, respectively. The quartz tube with the sample was removed from the horizontal furnace immediately after the specific reaction time. The masses of the samples were weighed after the product had cooled naturally to room temperature.

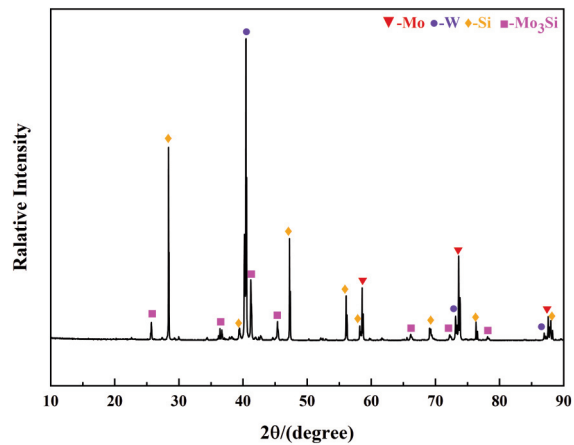


Figure 5. The XRD patterns of product with the raw materials of Mo, W and Si powders after reacting at 1150°C for 2 h

The weight loss rate W is defined as equation (12):

$$W_i = \frac{m_0 - m_i}{m_0} \quad (12)$$

where m_0 and m_i are the initial and final weights of the sample, respectively. According to reactions (2-3), and assuming that SiS has escaped completely from the sample, the mass loss of the experimental system is therefore the mass of SiS captured by CaO. Therefore, the theoretical weight loss rate W_∞ is about 39.85 %. The curve of the reaction extent varying with time can be drawn by the following equation:

$$X = \frac{W_i}{W_\infty} \quad (13)$$

The effects of the holding time on the reaction extent are shown in Figure 6. The value of X is 1 when the reaction is completed.

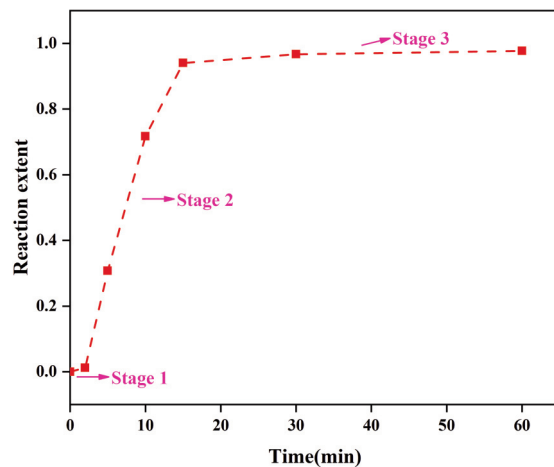


Figure 6. The curves of reaction extent X vs reaction time for sample MWS3



As depicted in Figure 6, three stages of the reaction process can be identified. The preliminary stage is a slow reaction stage in 0-2 min. The weight loss change can be neglected, and the value of X is only 0.012. This phenomenon could be caused by slow initial reaction rate between solid MoS_2 and solid Si. The second stage (2-15 min) is a rapid reaction stage. The reaction extent increases linearly and reaches 0.94 in 15 min. At this stage, the possible reaction is the gas-solid reaction among MoS_2 , W and SiS. The produced SiS_2 transfers to the surface of Si particles to react and produce SiS gas again to take part in the next round of MoS_2 formation process and sulfuration reaction of W. The third stage is the deep desulfurization stage. Only a small amount of reaction is still in progress. When the holding time is prolonged to 60 min, the reaction extent X is infinitely close to 1.

Figure 7 shows the XRD patterns of the products for samples MWS3 acquired after reacting at 1150°C for various holding times. It can be found that the main phase is $(\text{Mo,W})\text{Si}_2$, besides small amounts of WSi_2 and Si in the initial stage. This is in accordance with the low reaction extent after 5 min in the above analysis. The diffraction peaks of Si disappear and only the peaks of $(\text{Mo,W})\text{Si}_2$ and WSi_2 are observed when the reaction time is prolonged to 15 min, which is consistent with the fact that the reaction is basically completed after 15 min. After further extending the reaction time, there are no obvious changes in the XRD results except for the increase in the intensity of the diffraction peak of WSi_2 . It can be presumed that most of the MoSi_2 and WSi_2 were formed in the first 15 min of the reaction.

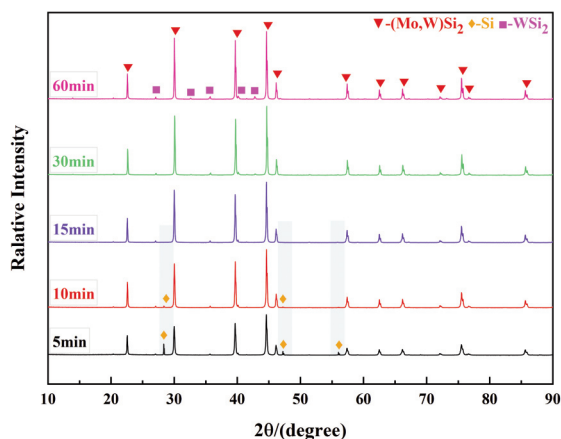


Figure 7. XRD patterns of the samples obtained at 1150°C for different durations

3.4. Residual sulfur content analysis

Due to the minor fraction of sulfide in the product, detecting the corresponding diffraction peaks by XRD

is difficult. To investigate the effect of reaction time on the residual sulfur content in product, the samples MWS3 fabricated at 1150°C for 15, 30, 60 and 120 min were examined using an infrared carbon-sulfur analyzer, and the corresponding results are present in Figure 8.

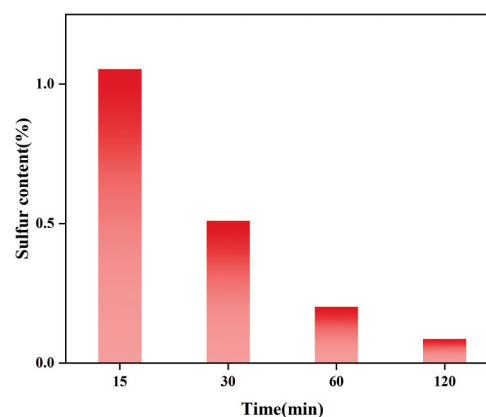


Figure 8. The residual sulfur contents (weight percentage) of the samples acquired at 1150°C for different times

Obviously, the residual sulfur content decreases with increasing duration. After reacting for 15 min, the residual sulfur content is 1.054 wt.%. When the reaction is prolonged to 30 min, the remaining sulfur content drops to 0.510 wt.%. After reacting for 60 min and 120 min, the residual sulfur content is further minimized to 0.202 wt.% and 0.087 wt.%, respectively, indicating that extending the holding time is beneficial to reduce the residual sulfur content. In fact, according to our previous research, the residual sulfur content can be further decreased by increasing the reaction temperature and prolonging the reaction time [35].

3.5. Microstructure and morphologies evolution

Figure 9 illustrates the FE-SEM images of the composite powders acquired at 1150°C for different times (5, 10, 30 and 120 min). Interestingly, the synthesized powders preserve the stacked sheet-like structure of the raw MoS_2 materials shown in Figure 1(A). Chang et al. [39] reported that ultra-fine MoSi_2 powders synthesized by silicothermic reduction of MoS_2 maintained the morphology, size, and sheet-like structure of MoS_2 . Moreover, a small number of blocky particles can be seen in Figures 9(A1) and (B1), which are marked with red circles. Combining Figure 1(C) and Figure 9 it can be assumed that these particles are the unreacted Si. However, they disappear after 30 and 120 minutes, as shown in Figures 9(C1) and (D1).

Figures 9(A2), (B2), (C2) and (D2) show the local, highly magnified views of (A1), (B1), (C1) and (D1),

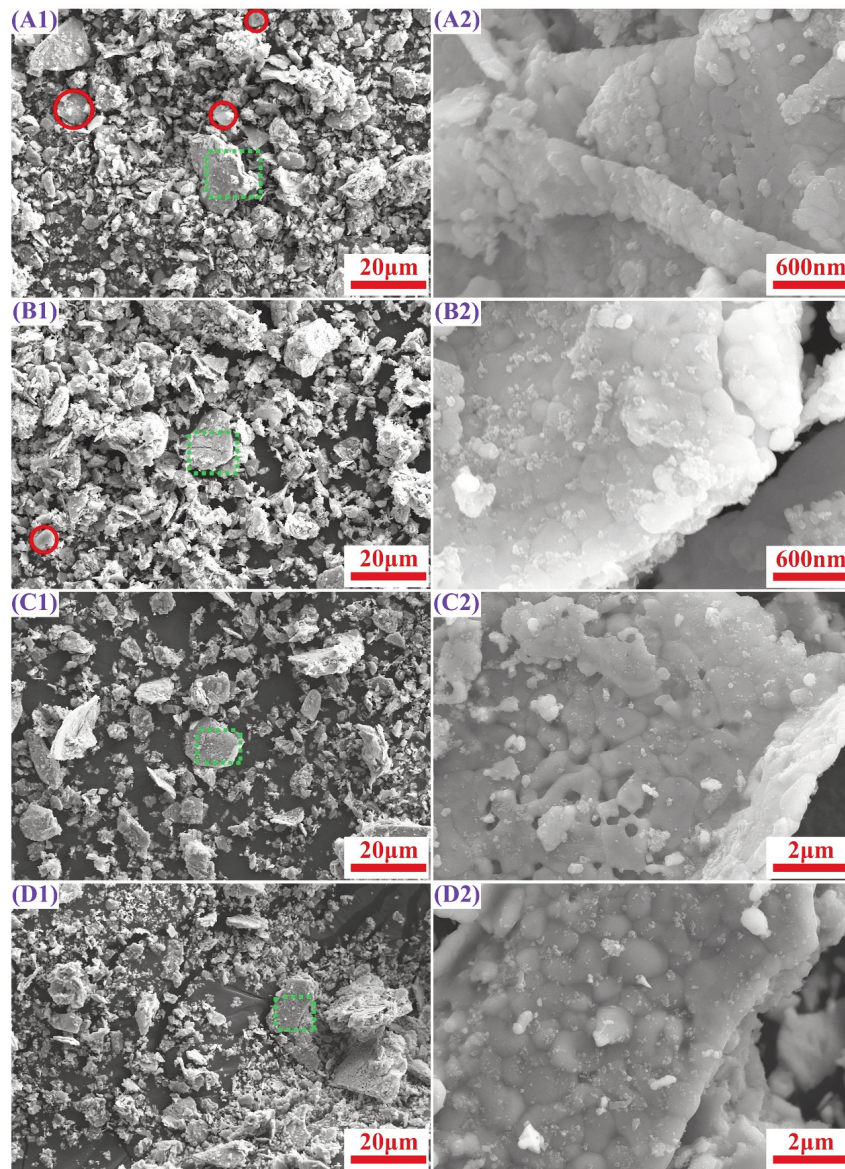


Figure 9. FE-SEM images of the samples MWS3 obtained at 1150 °C for various times: (A) 5 min; (B) 10 min; (C) 30 min; (D) 120 min

respectively. In particular, the acquired powder grains have a spherical or elliptical morphology and obvious sintering necks. The average grain size of the synthesized powder is about 300 nm, as seen in Figures 9(A2-B2). However, when the annealing time is prolonged to 60 min (Figure 9(C2)), the grain size increases significantly, with an average grain size of around 1 μm . Interestingly, the grain size does not change significantly when the annealing duration is prolonged to 120 min (Figure 9(D2)). It can be interpreted that the dependence of the grain size on the annealing time decreases when the holding time exceeds 60 min. On the whole, increasing the reaction time causes grain growth.

Figure 10 presents the results of the FE-SEM/EDS of the MWS3 samples obtained at 1150°C after various times (5, 10, 30 and 120 min). As shown in Figure 10(A), the elemental Mo map almost completely coincides with the elemental Si map, indicating the presence of MoSi_2 . However, there are accumulation zones (white circles) of Si in the elemental Si map but no enrichment of Mo or W, indicating that these regions are unreacted element Si. Moreover, element W is almost uniformly distributed, implying that the majority of W has been dissolved into MoSi_2 . It should be noted that there are some regions (red circle) where only W and Si are enriched. The red circle regions are WSi_2 , which does not

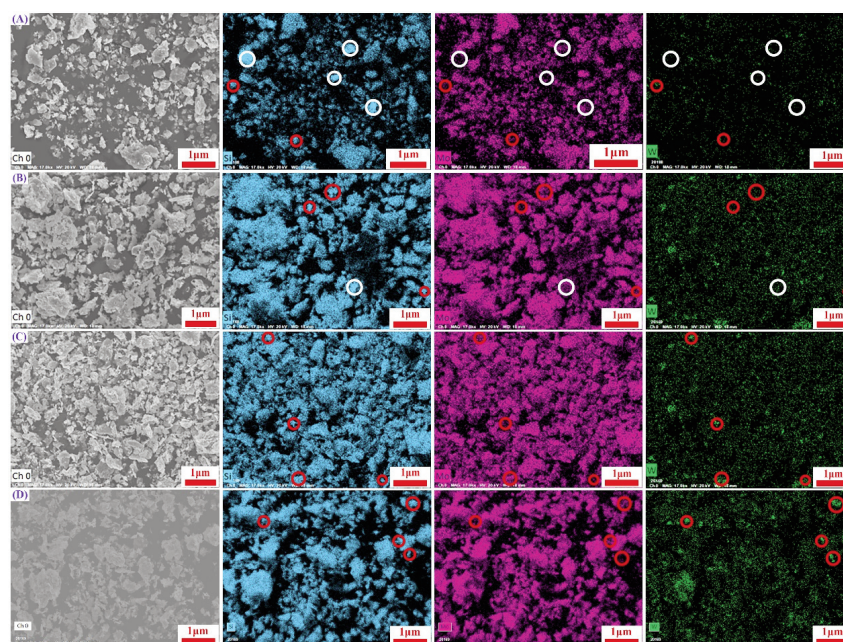


Figure 10. The morphology images of samples obtained at 1150 °C for different times (A) 5 min; (B) 10 min; (C) 30 min; (D) 120 min, and the corresponding EDS mapping distributions of Mo, W and Si elements

dissolve into MoSi_2 . The Si-enriched areas in Figure 10(B) are reduced, indicating that the amount of unreacted Si content has decreased. After reacting for 30 and 120 min, the independent Si-enriched regions are no longer present (Figures 10(C) and (D)), which is consistent with the XRD findings that the Si has been exhausted when the annealing duration is extended to 30 min. Figures 10(C) and (D) show the simultaneous enrichment of the elements Mo, W, and Si, and the elements W and Si, corresponding to tetragonal $(\text{Mo,W})\text{Si}_2$ and hexagonal WSi_2 , respectively.

4. Conclusions

In the present work, the $(\text{Mo,W})\text{Si}_2$ composite powder was successfully prepared using MoS_2 , W and Si powders as raw materials and lime as desulfurization agent. The main conclusions can be summarized as follows:

(1) The composite powder with the main phases of $(\text{Mo,W})\text{Si}_2$ and WSi_2 and a grain size of about 1 μm were obtained at 1150°C for 2 h.

(2) The residual sulfur content could be decreased to 0.084 wt.% after reacting at 1150°C for 120 min.

(3) The macro morphology and microstructure of the products were mainly inherited from the raw material MoS_2 .

(4) The formation of the gaseous intermediate product SiS changed the reaction from a solid-solid reaction to a gas-solid reaction, effectively accelerating the reaction process.

Acknowledgements

The authors gratefully acknowledge financial support from the State Key Laboratory of Advanced Metallurgy, University of Science and Technology Beijing, China.

Author's Contributions

Jia-Bing Huang: Methodology, Investigation, Writing - original draft. Guo-Hua Zhang: Resources, Supervision, Methodology, Writing - review & editing.

Data availability Statement

All data generated or analyzed during this study are included in this published article.

Conflict of interest

The authors declare that they have no conflict of interest.

References

- [1] J.J. Petrovic, Toughening strategies for MoSi_2 -based high temperature structural silicides, *Intermetallics*, 8(9-11) (2000) 1175-1182. [http://dx.doi.org/10.1016/s0966-9795\(00\)00044-3](http://dx.doi.org/10.1016/s0966-9795(00)00044-3)
- [2] W.Y. Lin, J.Y. Hsu, R.F. Speyer, Stability of molybdenum disilicide in combustion gas environments, *Journal of the American Ceramic Society*, 77(5) (1994) 1162-1168.



- <https://doi.org/10.1111/j.1151-2916.1994.tb05388.x>
- [3] R.G. Castro, J.R. Hellmann, A.E. Segall, D.L. Shelleman, Fabrication and testing of plasma-spray formed MoSi₂ and MoSi₂ composite tubes, MRS Online Proceedings Library (OPL), 322 (1993) 81. <https://doi.org/10.1557/PROC-322-81>
- [4] L. Zhang, Z.W. Tong, R.J. He, C. Xie, X.J. Bai, Y.Z. Yang, D.N. Fang, Key issues of MoSi₂-UHTC ceramics for ultra high temperature heating element applications: Mechanical, electrical, oxidation and thermal shock behaviors, Journal of Alloys and Compounds, 780 (2019) 156-163. <http://dx.doi.org/10.1016/j.jallcom.2018.11.384>
- [5] R. He, Z. Tong, K. Zhang, D. Fang, Mechanical and electrical properties of MoSi₂-based ceramics with various ZrB₂-20 vol% SiC as additives for ultra high temperature heating element, Ceramics International, 44(1) (2018) 1041-1045. <http://dx.doi.org/10.1016/j.ceramint.2017.10.043>
- [6] R. Wick-Joliat, S. Mauchle, R. Kontic, S. Ehrat, T. Hocker, D. Penner, MoSi₂/Al₂O₃/Feldspar Composites for Injection-Molded Ceramic Heating Elements, Advanced Engineering Materials, 23(9) (2021) 2100517. <https://doi.org/10.1002/adem.202100517>
- [7] S. Köbel, J. Plüschke, U. Vogt, T.J. Graule, MoSi₂-Al₂O₃ electroconductive ceramic composites, Ceramics international, 30(8) (2004) 2105-2110. <https://doi.org/10.1016/j.ceramint.2003.11.015>
- [8] H. Chen, Q. Ma, X. Shao, J. Ma, C. Wang, B. Huang, Microstructure, mechanical properties and oxidation resistance of Mo₅Si₃-Al₂O₃ composite, Materials Science and Engineering: A, 592 (2014) 12-18. <https://doi.org/10.1016/j.msea.2013.10.095>
- [9] M. Kermani, M. Razavi, M. R. Rahimipour, M. Zakeri, The effect of temperature on the in situ synthesis-sintering and mechanical properties of MoSi₂ prepared by spark plasma sintering, Journal of Alloys and Compounds, 585 (2014) 229-233. <https://doi.org/10.1016/j.jallcom.2013.09.125>
- [10] A.K. Bhattacharya, J.J. Petrovic, Hardness and Fracture Toughness of SiC-Particle-Reinforced MoSi₂ Composites, Journal of the American Ceramic Society, 74(10) (1991) 2700-2703. <https://doi.org/10.1111/j.1151-2916.1991.tb06828.x>
- [11] D.E. Alaman, N.S. Stoloff, Effect of ductile phase reinforcement morphology on toughening of MoSi₂, MRS Online Proceedings Library, 273(1) (1992) 247-252. <http://dx.doi.org/10.1557/PROC-273-247>
- [12] D.H. Carter, J.J. Petrovic, R.E. Honneu, W.S. Gibbs, SiC-MoSi₂ Composite, A Collection of Papers Presented at the 13th Annual Conference on Composites and Advanced Ceramic Materials, Part 2 of 2: Ceramic Engineering and Science Proceedings, 10(9/10) (1989) 1121-1129. <https://doi.org/10.1002/9780470310588.ch10>
- [13] D. Yi, C. Li, MoSi₂-ZrO₂ composites-fabrication, microstructures and properties, Materials Science and Engineering: A, 261(1-2) (1999) 89-98. [https://doi.org/10.1016/S0921-5093\(98\)01053-3](https://doi.org/10.1016/S0921-5093(98)01053-3)
- [14] H. Zhang, D. Wang, S. Chen, X. Liu, Toughening of MoSi₂ doped by La₂O₃ particles, Materials Science and Engineering A, 345(1-2) (2003) 118-121. [https://doi.org/10.1016/S0921-5093\(02\)00455-0](https://doi.org/10.1016/S0921-5093(02)00455-0)
- [15] A. Newman, S. Sampath, H. Herman, Processing and properties of MoSi₂-SiC and MoSi₂-Al₂O₃, Materials Science and Engineering: A, 261(1-2) (1999) 252-260. [https://doi.org/10.1016/S0921-5093\(98\)01073-9](https://doi.org/10.1016/S0921-5093(98)01073-9)
- [16] M. Patel, J. Subramanyam, V. Prasad, Synthesis and mechanical properties of nanocrystalline MoSi₂-SiC composite, Scripta Materialia, 58(3) (2008) 211-214. <https://doi.org/10.1016/j.scriptamat.2007.09.038>
- [17] M. Panneerselvam, A. Agrawal, K.J. Rao, Microwave sintering of MoSi₂-SiC composites, Materials Science and Engineering A, 356(1-2) (2003) 267-273. [https://doi.org/10.1016/S0921-5093\(03\)00140-0](https://doi.org/10.1016/S0921-5093(03)00140-0)
- [18] Y. Suzuki, P. Morgan, K. Niihara, Improvement in mechanical properties of powder-processed MoSi₂ by the addition of Sc₂O₃ and Y₂O₃, Journal of the American Ceramic Society, 81(12) (1998) 3141-2149. <https://doi.org/10.1111/j.1151-2916.1998.tb02749.x>
- [19] G.Y. Lu, R. Lederich, W. Soboyejo, Residual stresses and transformation toughening in MoSi₂ composites reinforced with partially stabilized zirconia, Materials Science and Engineering: A, 210(1-2) (1996) 25-41. [https://doi.org/10.1016/0921-5093\(95\)10075-X](https://doi.org/10.1016/0921-5093(95)10075-X)
- [20] R. Rao, Effect of minor alloying with Al on oxidation behaviour of MoSi₂ at 1200 °C, Materials Science and Engineering: A, 260(1-2) (1999) 146-160. [https://doi.org/10.1016/S0921-5093\(98\)00972-1](https://doi.org/10.1016/S0921-5093(98)00972-1)
- [21] X. Wang, P.Z. Feng, F. Akhtar, J. Wu, W. Liu, Y. Qiang, Z. Wang, Effects of tungsten and aluminum additions on the formation of molybdenum disilicide by mechanically-induced self-propagating reaction, Journal of Alloys and Compounds, 490(1-2) (2010) 388-392. <http://dx.doi.org/10.1016/j.jallcom.2009.09.189>
- [22] G.J. Zhang, X.M. Yue, T. Watanabe, Addition effects of aluminum and in situ formation of alumina in MoSi₂, Journal of Materials Science, 34(5) (1999) 997-1001. <https://doi.org/10.1023/A:1004583625750>
- [23] Y. Harada, Y. Murata, M. Morinaga, Solid solution softening and hardening in alloyed MoSi₂, Intermetallics, 6(6) (1998) 529-535. [https://doi.org/10.1016/S0966-9795\(97\)00103-9](https://doi.org/10.1016/S0966-9795(97)00103-9)
- [24] H. Zhang, P. Chen, J. Yan, S. Tang, Fabrication and wear characteristics of MoSi₂ matrix composite reinforced by WSi₂ and La₂O₃, International Journal of Refractory Metals and Hard Materials, 22(6) (2004) 271-275. <https://doi.org/10.1016/j.ijrmhm.2004.09.002>
- [25] F. Chen, J. Xu, Y. Liu, L. Cai, In situ reactive spark plasma sintering of WSi₂/MoSi₂ composites, Ceramics international, 42(9) (2016) 11165-11169. <https://doi.org/10.1016/j.ceramint.2016.04.023>
- [26] S. Bose, Engineering aspect of creep deformation of molybdenum disilicide, Materials Science and Engineering: A, 155(1-2) (1992) 217-225. [https://doi.org/10.1016/0921-5093\(92\)90328-X](https://doi.org/10.1016/0921-5093(92)90328-X)
- [27] R.B. Schwarz, S.R. Srinivasan, J.J. Petrovic, C.J. Maggiore, Synthesis of molybdenum disilicide by mechanical alloying, Materials Science and Engineering: A, 155(1-2) (1992) 75-83. [https://doi.org/10.1016/0921-5093\(92\)90314-Q](https://doi.org/10.1016/0921-5093(92)90314-Q)
- [28] S. Zamani, H.R. Bakhsheshi-Rad, M.R.A. Kadir, M.R. M. Shafiee, Synthesis and kinetic study of (Mo, W)Si₂-WSi₂ nanocomposite by mechanical alloying, Journal of alloys and compounds, 540 (2012) 248-259. <https://doi.org/10.1016/j.jallcom.2012.06.072>
- [29] S. Jo, G.W. Lee, J.T. Moon, Y.S. Kim, On the formation of MoSi₂ by self-propagating high-temperature synthesis, Acta Materialia, 44(11) (1996) 4317-4326. [https://doi.org/10.1016/1359-6454\(96\)00106-1](https://doi.org/10.1016/1359-6454(96)00106-1)



- [30] A.M. Nartowski, I.P. Parkin, Solid state metathesis synthesis of metal silicides; reactions of calcium and magnesium silicide with metal oxides, *Polyhedron*, 21(2) (2002) 187-191.
[https://doi.org/10.1016/S0277-5387\(01\)00974-3](https://doi.org/10.1016/S0277-5387(01)00974-3)
- [31] J. Yan, J. Xu, Y. Wang, L.F. Liu, Preparation of agglomerated powders for air plasma spraying MoSi₂ coating, *Ceramics International*, 41(9) (2015), 10547-10556.
<https://doi.org/10.1016/j.ceramint.2015.04.149>
- [32] L. Wang, G.H. Zhang, J. Dang, K.C. Chou, Oxidation roasting of molybdenite concentrate, *Transactions of Nonferrous Metals Society of China*, 25(12) (2015) 4167-4174.
[https://doi.org/10.1016/S1003-6326\(15\)64067-5](https://doi.org/10.1016/S1003-6326(15)64067-5)
- [33] J. Dang, G.H. Zhang, K.C. Chou, R.G. Reddy, Y. He, Y. Sun, Kinetics and mechanism of hydrogen reduction of MoO₃ to MoO₂, *International Journal of Refractory Metals and Hard Materials*, 41 (2013) 216-223.
<https://doi.org/10.1016/j.ijrmhm.2013.04.002>
- [34] J. Dang, G. H. Zhang, K.C. Chou, Study on kinetics of hydrogen reduction of MoO₃, *International Journal of Refractory Metals and Hard Materials*, 41 (2013) 356-362. <https://doi.org/10.1016/j.ijrmhm.2013.05.009>
- [35] G.D. Sun, G.H. Zhang, Study on the preparation of molybdenum silicides by the silicothermic reduction of MoS₂, *Journal of Alloys and Compounds*, 728 (2017) 295-306.
<http://dx.doi.org/10.1016/j.jallcom.2017.08.299>
- [36] H.Q. Chang, G.H. Zhang, K.C. Chou, A novel sulfur-emission free route for preparing ultrafine MoSi₂ powder by silicothermic reduction of MoS₂, *Journal of the American Ceramic Society*, 104(12) (2021) 6092-6099. <https://doi.org/10.1111/jace.17994>
- [37] G.D. Sun, K.F. Wang, C.M. Song, G.H. Zhang, A low-cost, efficient, and industrially feasible pathway for large scale preparation of tungsten nanopowders, *International Journal of Refractory Metals and Hard Materials*, 78 (2019) 100-106.
<https://doi.org/10.1016/j.ijrmhm.2018.08.013>
- [38] H.Q. Chang, H.Y. Wang, G.H. Zhang, K.C. Chou, Controllable syntheses of Mo₅Si₃ and Mo₃Si by silicothermic reduction of MoS₂ in the presence of lime, *Ceramics International*, 48(6) (2022) 7815-7826.
<http://dx.doi.org/10.1016/j.ceramint.2021.11.329>
- [39] H.Q. Chang, G.H. Zhang, Mechanism and kinetics of silicothermic reduction of MoS₂ for preparing ultrafine grain MoSi₂ powder, *Powder Technology*. 414 (2023) 118102.
<https://doi.org/10.1016/j.powtec.2022.118102>
- [40] W.P. Davey, Precision measurements of the lattice constants of twelve common metals, *Physical Review*, 25(6) (1925) 753.
<https://doi.org/10.1103/PhysRev.25.753>
- [41] E. Ström, Y. Cao, Y.M. Yao, Low temperature oxidation of Cr-alloyed MoSi₂, *Transactions of Nonferrous Metals Society of China*, 17(6) (2007) 1282-1286.
[https://doi.org/10.1016/S1003-6326\(07\)60263-5](https://doi.org/10.1016/S1003-6326(07)60263-5)
- [42] D.E. Alman, R.D. Govier, Influence of Al additions on the reactive synthesis of MoSi₂, *Scripta Materialia*, 34(8) (1996) 1287-1293.
[https://doi.org/10.1016/1359-6462\(95\)00655-9](https://doi.org/10.1016/1359-6462(95)00655-9)
- [43] J. Subrahmanyam, R.M. Rao, Combustion synthesis of MoSi₂-WSi₂ alloys, *Materials Science and Engineering: A*, 183(1-2) (1994) 205-210.
[https://doi.org/10.1016/0921-5093\(94\)90904-0](https://doi.org/10.1016/0921-5093(94)90904-0)
- [44] A. Stergiou, P. Tsakiroopoulos, The intermediate and high-temperature oxidation behaviour of (Mo,X)Si₂ (X= W, Ta), intermetallic alloys, *Intermetallics*, 5(2) (1997) 117-126.
[https://doi.org/10.1016/S0966-9795\(96\)00074-X](https://doi.org/10.1016/S0966-9795(96)00074-X)
- [45] W. Lin, L. Chen, Localized epitaxial growth of tetragonal and hexagonal WSi₂ on (111) Si, *Journal of Applied Physics*, 58(4) (1985) 1515-1518.
<https://doi.org/10.1063/1.336308>
- [46] D. Ovalı, D. Ağaoğulları, M.L. Öveçoğlu, Room-temperature synthesis of tungsten silicide powders using various initial systems, *International Journal of Refractory Metals and Hard Materials*, 82 (2019) 58-68. <https://doi.org/10.1016/j.ijrmhm.2019.03.028>
- [47] D. Ovalı, D. Ağaoğulları, M.L. Öveçoğlu, Characterization of SiO₂-encapsulated WSi₂/W₅Si₃ nanoparticles synthesized by a mechanochemical route, *Ceramics International*, 44(8) (2018) 9442-9453.
<https://doi.org/10.1016/j.ceramint.2018.02.161>



SINTEZA ULTRAFINIH (Mo,W) Si₂ KOMPOZITNIH PRAHOVA IZ KONCENTRATA MOLIBDENA VISOKE ČISTOĆE

J.-B. Huang, G.-H. Zhang*

Glavna državna laboratorija za naprednu metalurgiju, Univerzitet nauke i tehnologije u Pekingu, Peking, Kina

Apstrakt

(Mo,W)Si₂ kompozitni prahovi veličine zrna oko 1 μm sintetisani su na 1150°C u trajanju od 2 h. Kao sirovine su korišćeni koncentrat molibdena visoke čistoće (sa glavnom komponentom MoS₂), prah W i Si, a kao sredstvo za odsumporavanje je korišćen kreč. Grafitni filc je položen između kompakta (napravljenog od MoS₂, W i Si) i kreča da bi se olakšalo odvajanje proizvedenih kompozitnih prahova od proizvoda odsumporavanja. Procenjavani su fazni sastav, evolucija mikrostrukture i sadržaj zaostalog sumpora tokom reakcije silikotermalne redukcije. Eksperimentalni rezultati su pokazali da se reakcija može završiti nakon reakcionog vremena od 2 sata na temperaturi od 1150°C, a sadržaj zaostalog sumpora u proizvodu je bio 0,087 tež.%. Zaključeno je da su interakcije između Si i međuproizvoda SiS i SiS₂ ključne za pripremu (Mo,W)Si₂ kompozitnih prahova na niskim temperaturama. Proces pripreme se može podeliti u tri faze: reakcije u čvrstom stanju između MoS₂, W i Si da bi se dobili MoSi₂, WSi₂ i gasoviti SiS; reakcija gas-čvrsto između MoS₂, W i gasovitog SiS za stvaranje MoSi₂, WSi₂ i gasovitog SiS₂; i reakcija gas-čvrsto između gasovitog SiS₂ i Si da bi se formirao SiS gas. Ovim postupkom kratkog toka, fino zrnasti (Mo,W)Si₂ kompozitni prahovi se mogu proizvesti po niskoj ceni na niskoj temperaturi, što ima veliki potencijal primene.

Ključne reči: Molibden disilicid; Volfram disilicid; Kompozitni prahovi; Silikotermalna redukcija

